Tree Ring α-Hemicellulose Analysis of Fossilized Pliocene Wood from Ellesmere Island, Canada, for the Identification of Metal Oxide Contamination

Senior Thesis
Submitted in partial fulfillment of the requirements for the
Bachelor of Science Degree
At The Ohio State University

By

Brendon J. Mock
The Ohio State University
2015

Approved by

Joel D. Barker, Advisor
School of Earth Sciences

TABLE OF CONTENTS

Abstract

The northernmost known boreal forest from the Late Pliocene epoch is located in Quttinirpaaq National Park, Nunavut, Canada (81.5°N). The Pliocene epoch has attracted significant attention as a proxy for global climate change predicted for the 21st century. Tree ring analysis, in combination with isotope analysis of plant tissue (cellulose), has been used to determine ancient climate conditions during the time that the trees grew. In this study, we examine the tree ring width and ring width distribution from three preserved tree trunks (*Betula* and *Picea*) from this Arctic Pliocene forest deposit (Ekblaw A). Further, we examine the purity of α-hemicellulose extracted from these growth rings to detect the presence of metal oxides (FeO) in the extract using FTIR and SEM/EDX spectroscopy. The presence of FeO may compromise oxygen stable isotope analyses that are performed on α-hemicellulose.

Results indicate that the trees from the Ekblaw A site grew slowly (mean ring width = 0.26 mm, range = 0.5mm–1.7mm). This growth rate is lower than those reported for other Arctic Pliocene sites. $\delta^{18}O$ values of α-hemicellulose extracted from growth rings range from 11.48‰ VSMOW to 20.40‰ VSMOW. Some growth rings report $\delta^{18}O$ values that are lower than those reported from other Arctic sites (mean = 19.5‰ VSMOW, range = 16.0‰ VSMOW-24‰ VSMOW). Examination of α-hemicellulose extracts indicates that no FeO is present in the samples and suggest that trees from the Ekblaw A site grew under different climate conditions than other Pliocene forests in the Arctic.

Acknowledgements

My sincerest thanks is given to Dr. Joel Barker for his guidance, attentiveness, expertise, and patience during this endeavor. I have never been academically inclined and he willingly took on a challenge by agreeing to be my mentor. Without him, I am certain that I would have produced a less competent thesis. I would also like to thank Doctoral Candidate Oliver Wigmore of the Department of Geography for giving me a chance to help him with his research, even if it did not work out in the end. I'd like to thank George Grant for his help organizing my thoughts and his input toward ideas for future work for this thesis. I'd like to express my gratitude to Bethany Wellen and Spencer Day from Ohio State's Chemistry Department for their assistance gathering data from the FTIR spectrometer, along with Dr. Sue Welch for running SEM/EDX analysis on our samples. I'd like to thank the National Science Foundation's Division of Arctic Sciences for their issue of grant # 1026177 (2010) that funded the expedition to Ellesmere Island. Finally, I'd like to thank Dr. Anne Carey for introducing me to previously unknown cooking blogs and for patiently awaiting the submission of this thesis without pressuring me for a version that was not yet complete.

To my friends, I want to express my gratitude for always being there when I needed an ear to complain to and for helping me to laugh my way through these last four years.

Furthermore, I would like to thank Dr. Terry Wilson, Dr. Cristina Millan, Dr. Shelley Judge, Dr. Dan Kelley, and all my classmates (especially John Jones, Megan Mave, and Micheala Wells; listed alphabetically to avoid favoritism) for contributing to a wonderful six weeks in Utah. The experience and friendships developed during field camp will stay with me for the remainder of my life and are what convinced me that I may not have made a mistake choosing this major.

I'd like to feverishly extend my gratitude to my mother, Andrea Mock, for all of her encouragement and love over the difficult last 10 years of my life, and to my father, James Mock, for sacrificing so much to provide me and my siblings with the safe and comfortable upbringing that I so frequently took for granted.

And finally, and with the utmost respect and love, I would like to thank Ashton Bishop for her unwavering support throughout our time together, despite all my many flaws.

1. Introduction

Earth's climate has changed throughout history. Temperature measurements over the last 130 years indicate that the planet is experiencing a rise in its average annual temperature with a predicted continued rise of 2-3 °C over the next 75 years (Pachauri et al., 2014). This increase is largely attributed to the growing concentration of greenhouse gases (GHGs), such as carbon dioxide (CO_2), in the Earth's atmosphere. Increased atmospheric GHG concentrations amplify Earth's greenhouse effect, resulting in increased temperature on the Earth's surface and the troposphere (Karl and Trenberth, 2003).

According to the latest readings from the Mauna Loa Observatory in Hawaii, the current atmospheric CO_2 concentration is 401.18 ppm (06 December 2015). The pre-Industrial Revolution CO_2 concentration was 272 ppm and corresponded with an average global temperature that was 0.85 °C lower than today (Holland and Bitz, 2003). However, the average temperature in the northern polar region has increased 2.97 °C over the same time due to so-called "polar amplification" that causes polar temperatures to increase at a rate up to 4.5 times faster than the global average (Holland and Bitz, 2003).

During the Pliocene epoch (2.6-5.3 Ma), global average temperature was 2-3 °C warmer than at present and atmospheric CO_2 levels fluctuated around 400 ppm; values that are within the range of predicted conditions for the 21st century (Davis et al., 2010). If global temperature increases 2-3 °C in the next century due to the rising GHG concentrations, a surge in Arctic temperature of

up to 13.5 °C could be observed (Holland and Bitz, 2003). Predicted global average temperature and atmospheric CO_2 concentrations are similar to those of the Pliocene epoch, and because of this, Pliocene deposits have been used as a proxy for conditions that might exist at the end of the 21st century (Csank et al., 2011).

While the distribution of Arctic landmasses during the Pliocene is similar to that of today (Knutz et al., 2015), the Pliocene Arctic ecosystem was much different. Average polar temperatures were 7-15 °C warmer than temperatures that immediately preceded the Industrial Revolution (Csank et al., 2011) and boreal forests extended to the Arctic Ocean. Current treeline rarely extends north of the Arctic Circle (Fig. 1; Serreze et al., 2000).

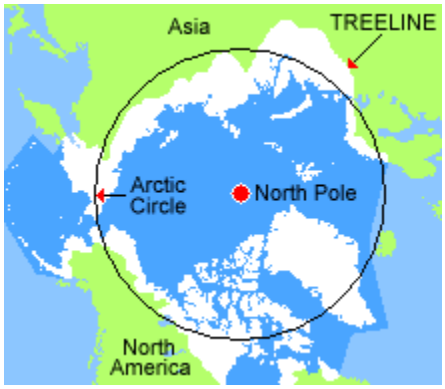

Figure 1. Present treeline and outline of the Arctic Circle.

The remains of these Pliocene forests, as preserved in sedimentary deposits, have been the subject of studies that seek to determine a temperature range for the Pliocene Arctic using the ratios of the stable isotopes of oxygen in α-hemicellulose extracts from non-mineralized (mummified) wood. However, the use of stable isotopes from α-hemicellulose extracts is subject to

misinterpretation due to the presence of metal oxides that selectively retain the heavier isotope and bias the reported results.

We identified the northernmost fossilized forest deposit in North America (Fig 2). Herein, we examine tree trunk samples for growth characteristics and examine α-hemicellulose from growth rings in these tree trunks to determine if the presence of metal oxides (FeO) may affect the oxygen isotope ratio of these trees and undermine their suitability for use in calculating temperatures in the Arctic during the Late Pliocene.

2. Methods

Samples of a variety of exposed tree species were taken from a Pliocene deposit (hereafter referred to as Ekblaw A), located on Ellesmere Island, Canada, in Quttinirpaaq National Park (81°40'N, 76°14'W) on two separate expeditions to the area during the summers of 2009 and 2010. A shovel was used to unearth buried mummified wood. A handsaw was used to remove portions of the trunks and these samples were wrapped in black garbage bags and sent back to The Ohio State University with minimal exposure to light.

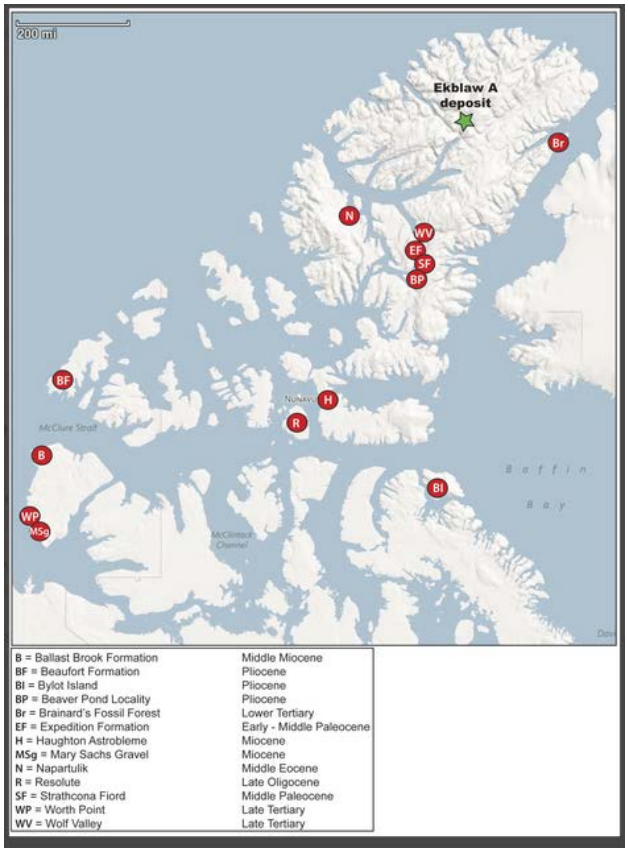

Figure 2. Map of the northernmost tip of Nunavut, Canada. Ekblaw A collection site denoted by star symbol.

The mummified wood specimens were sub-sampled using a fine toothed saw to cut the wood into transverse disks, which were polished using fine grade sandpaper. Tree genus identification was determined by morphological characteristics and ring number and ring width was measured to a detection limit of 0.05 mm using a stereo microscope and micro ruler. In order to use the tree rings from the samples to calculate the minimum age of the trees, we had to make the assumption that the ring count was continuous (Hughes et al., 1999).

Extraction of α-hemicellulos followed Loader et al. (1997). Select tree rings were sampled using a rotary scalpel attached to a drill until 0.30 – 0.35 mg had been collected. In order to remove carbohydrates from the samples, the shavings were placed in beakers containing a solution as prescribed by Loader et al. (1997; see Table 1) and the beakers were placed in an ultrasonic bath at ~70 °C under maximum power conditions for 4 hours. Acetic acid and sodium chlorite reagents were added to the beakers in the ultrasonic bath after every hour. The solution was then removed from the beakers by vacuum filtration and the shavings were washed in hot deionized water followed by cold deionized water. The shavings were then placed in a beaker with 10% (w/v) sodium hydroxide and returned to the ultrasonic bath, now at ~80 °C, for 45 minutes. The samples were removed and washed again with sub room temperature deionized water and then placed in another beaker containing 17% (w/v) sodium hydroxide. The third beaker was again placed in the ultrasonic bath for an additional 45 minutes, this time at room temperature.

The α-hemicellulose was then removed from the sodium hydroxide solution by vacuum filtration and washed with 17% (w/v) sodium hydroxide and deionized water and then with 1% (w/v) hydrochloric acid. Lastly, cold deionized water was used to flush out all remaining reagents until the α-hemicellulose was neutral. The α-hemicellulose was then dried in a vacuum oven at 40 °C for 4 hours.

Table 1
Reagent quantities per gram of shavings as described by Loader et al., (1997).

Reagent	Quantity of reagent
Wood shavings	1.0 g
Deionized water	175 ml
Sodium chlorite (per addition)	2.5 g
Acetic acid (per addition)	1.7 ml
10% (w/v) sodium hydroxide	75 ml
17% (w/v) sodium hydroxide	67 ml

The extracted samples were analyzed at the Environment and Natural Resources Institute Stable Isotope Laboratory, University of Alaska Anchorage, for $\delta^{18}O$ using a Thermo Finnigan TC/EA coupled with a Conflo III interface to a Thermo Finnigan Delta Plus XL mass spectrometer in continuous flow mode. Isotope values are reported relative to Vienna Standard Mean Ocean Water (VSMOW).

The possible presence of iron oxides (FeO) in the extracts was evaluated for select samples that reported abnormal $\delta^{18}O$ values using Fourier Transform Infrared (FTIR) spectroscopy and scanning electron microscopy coupled with energy dispersive X-ray spectroscopy (SEM/EDX). Two samples that displayed $\delta^{18}O$ levels outside of the norm as described by Csank et al. (2011) were

examined for the presence of FeO and one sample that displayed “typical” levels was examined.

To prepare for analysis by FTIR and SEM/EDX, the three chosen α-hemicellulose samples were ground into powder by mortar and pestle. First, a background spectrum was collected and converted to frequency data by inverse Fourier transform. Small portions of the samples were then fixed in place by skews for measurement and scanned in transmission mode. A single-beam spectrum of each sample was taken and the background frequency datum was removed to produce a spectrum composed of only the sample.

Following FTIR analysis, portions of the remaining α-hemicellulose extracts were prepared for inspection by SEM/EDX. Small amounts of the samples were fixed to double stick, electrically conductive carbon tape and mounted to pegs. In order for the SEM/EDX to produce images, the α-hemicellulose was coated with an electrically conductive material (graphite). The pegs were placed inside of a sputter coater, a plasma chamber with low discharge capability, in order to cover the surface of the samples with a thin layer of metal (<10 nanometers). The pegs were placed inside the vacuum chamber of the SEM/EDX and images and EDX spectrums were taken, with focus on detection of FeO granules.

3. Results

3.1 Tree Ring Analysis

Three tree trunks were chosen for age determination, ring width measurements, and genus classification. Growth statistics for each of the tree trunks included a collective average width of 0.26 mm, a maximum thickness of 1.7 mm, and a minimum detection limit of 0.05 mm (Table 2).

Table 2
Growth statistics for 3 tree trunks from the Ekblaw A site.

	09-6B	10-02	10-06
Genus	*Betula*	*Picea*	*Betula*
Age* (yrs)	>54	>104	>106
Avg. ring width (mm)	0.42	0.21	0.12
Range (mm)	0.1-1.7	0.05-1.5	0.05-0.6
Standard deviation	0.247	0.192	0.135
Mean sensitivity	0.489	0.254	0.121

*Age counting began at innermost ring. Minimum age is presented because the tree rings at the outer edge of the trunk were spaced too closely to allow the differentiation of separate tree rings.

Sample 09-6B exhibited 54 measurable rings (Fig. 3). The average growth rate is 0.43 mm/year and the ring width generally decreases toward the outer edges of the tree trunk. The peak growth rate occurs at ring 29 and shows a growth of 1.7 mm during that year. The minimum growth of the tree, 0.1 mm-0.2 mm/year, occurs at four periods throughout this tree's lifespan, at rings 6, 21, 38, and 52 (Fig. 3).

Sample 10-02 exhibited 104 measurable rings ranging in width from the minimum detection limit of 0.05 mm (rings 14, 23, 24, 50, 51, 98, 99) to 1.5

mm (ring 68; Fig. 4). The average growth of each ring is 0.21 mm and there is a slight increase across the sample's lifespan (Fig. 4).

Sample 10-06 exhibited 106 measureable rings (Fig. 5). The peak growth of 0.6 mm occurs at the 43rd tree ring. The minimum measureable growth rate of 0.05 mm occurs 28 times throughout its lifespan and the average ring width is 0.12 mm (Fig. 5) and the ring width generally decreases toward the outer edges of the tree trunk.

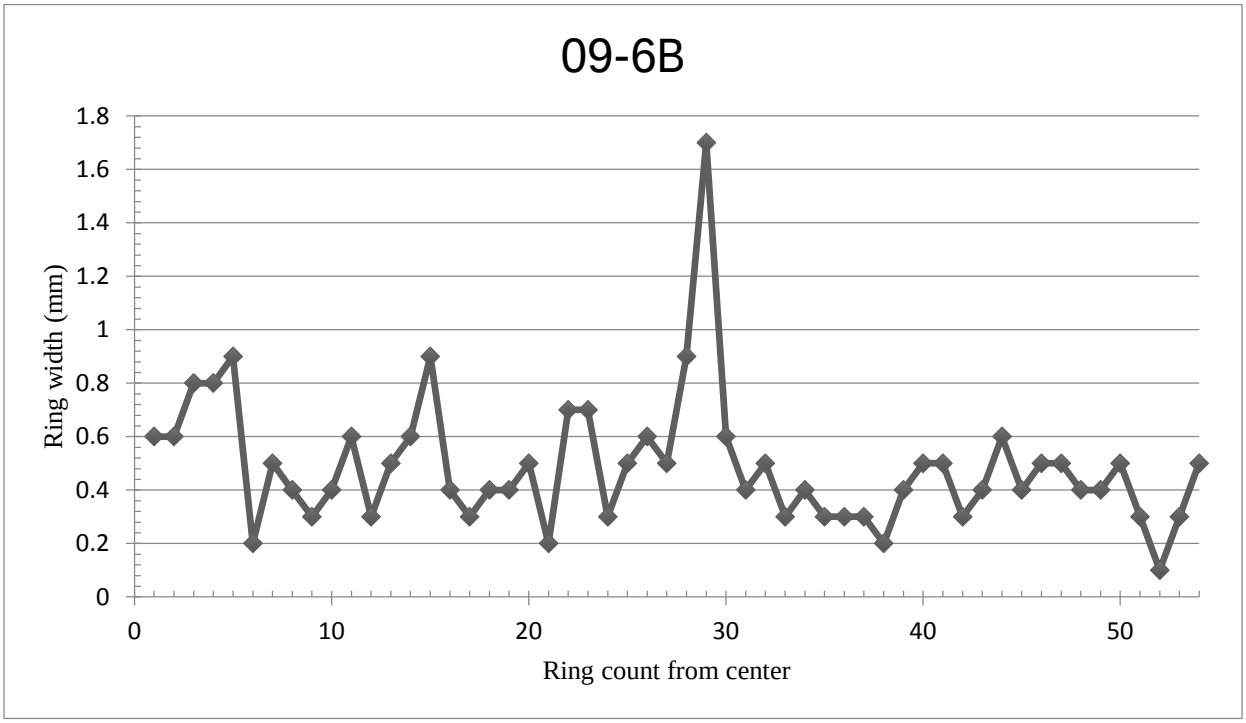

Figure 3. Ring width measurements from sample 09-6B showing 54 years of growth.

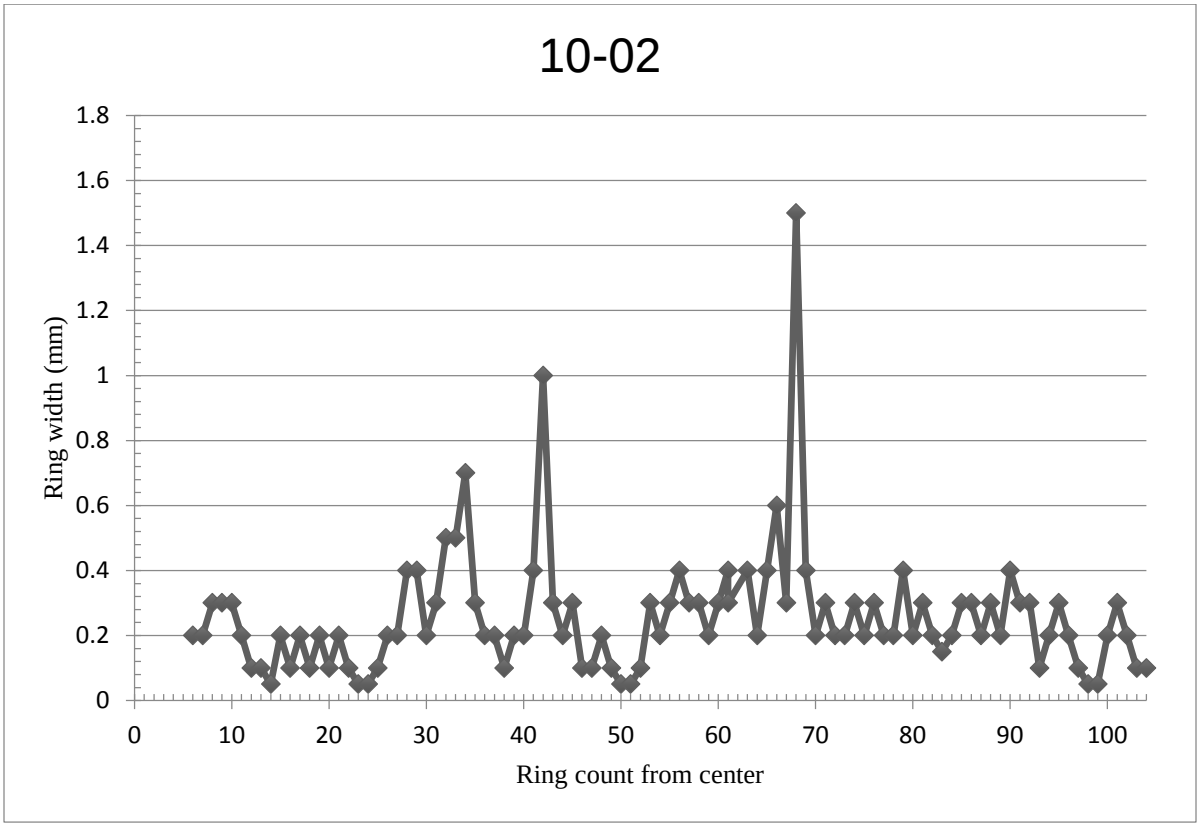

Figure 4. Ring width measurements from sample 10-02 showing 97 years of growth.

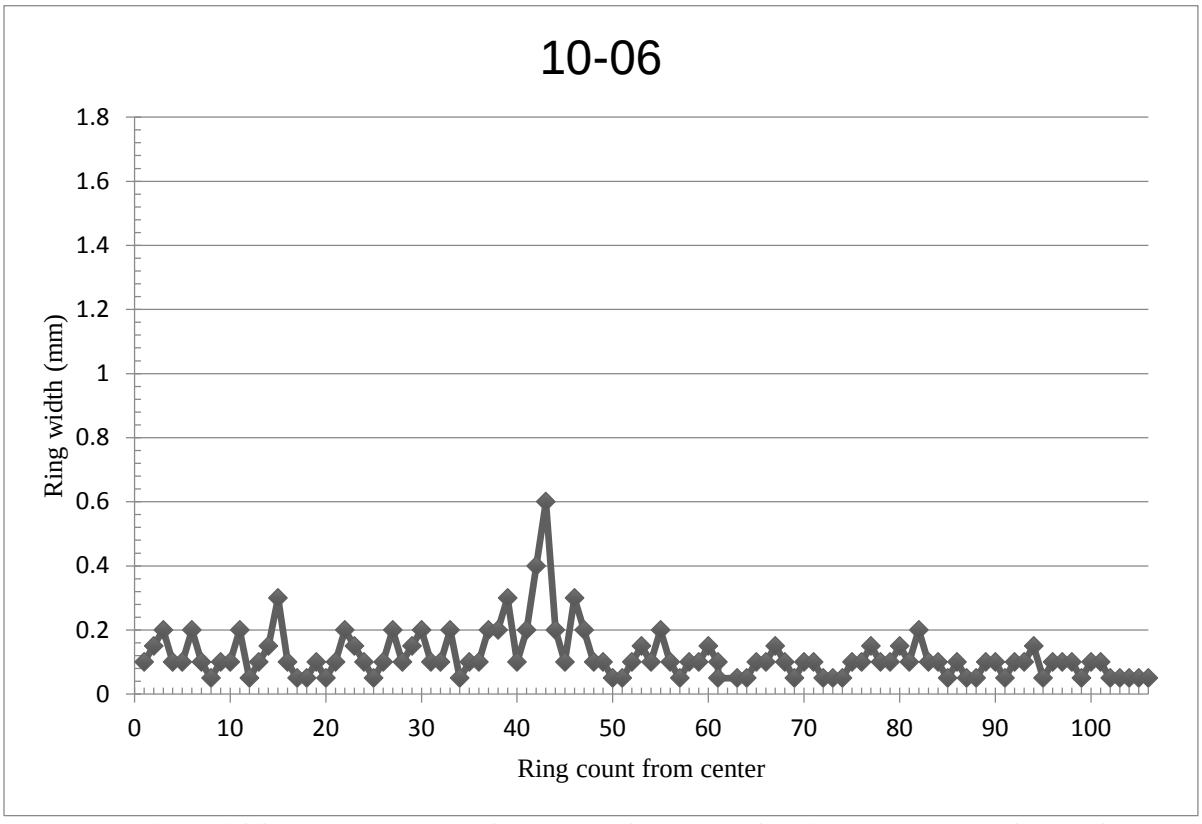

Figure 5. Ring width measurements from sample 10-06 showing 104 years of growth.

Because of similarities displayed by the samples in terms of ring width (e.g. regions surrounding ring 29 in sample 09-6B, ring 68 in sample 10-02, and ring 43 in sample 10-06), a correlation matrix (Table 3) was constructed to determine if the samples lived at the same point in time as indicated by similarities in growth. By centering the peak growth year of each sample and evaluating the bordering year (± 10 years; Fig. 6) we are able to show that the 3 sample trees did not share concurring lifespans.

Table 3
Correlation matrix of ring width measurements around peak growth year (±10yrs)

	09-6B Ring Width	10-02 Ring Width	10-06 Ring Width
09-6B Ring Width	1		
10-02 Ring Width	0.84	1	
10-06 Ring Width	0.81	0.72	1

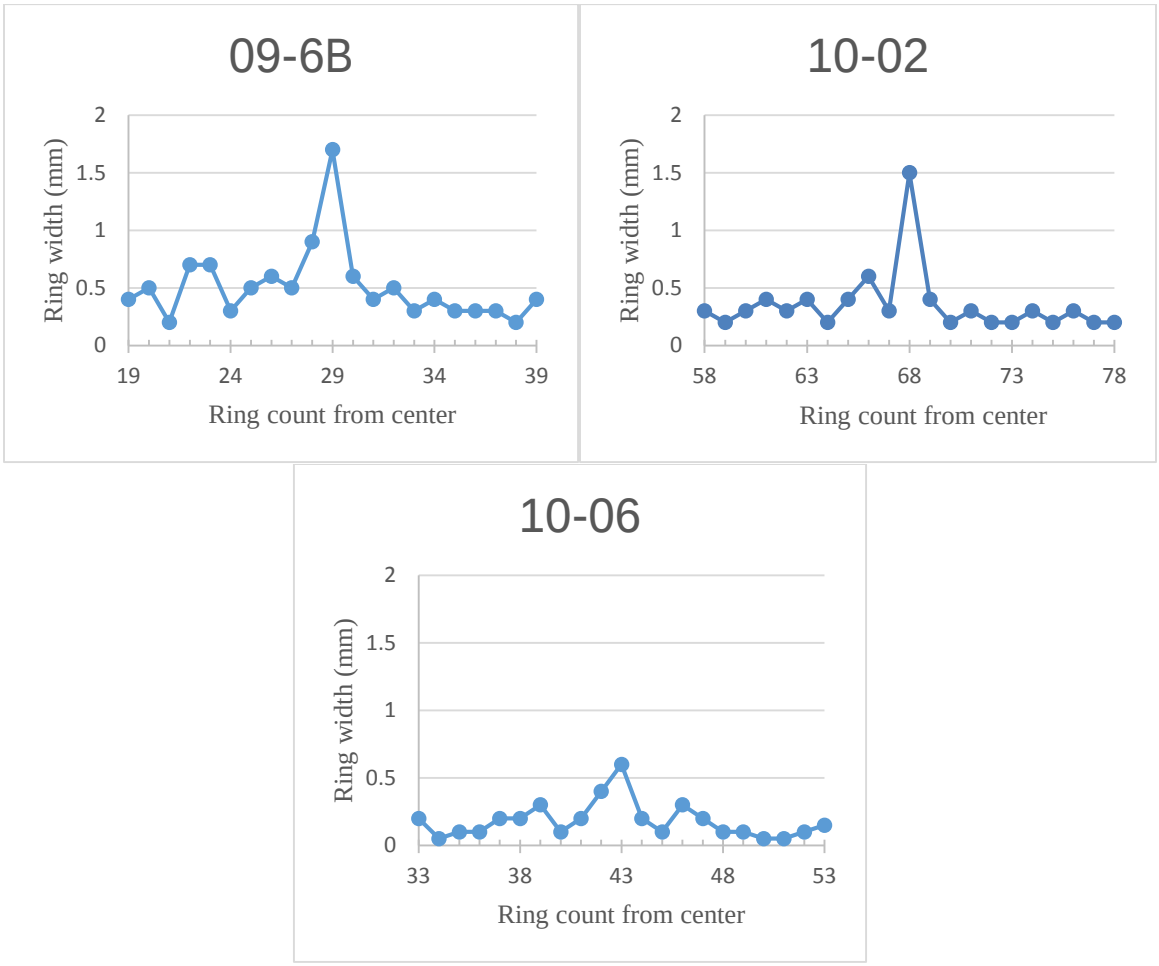

Figure 6. Correlated graphs of the samples with peak growing year centered on the X-axis.

3.2 Stable Isotope Analysis

The α-hemicellulose extracts from 09-6B produces $\delta^{18}O$ values ranging from 11.48‰ to 15.31‰ VSMOW with an average of 14.33‰ VSMOW. There is a decrease in the $\delta^{18}O$ value of the 12th tree ring. Sample 10-02 is shown to produce a range of $\delta^{18}O$ values from 14.00‰ to 20.39‰ VSMOW with an average of 18.15‰ VSMOW. Sample 10-06 is shown to produce $\delta^{18}O$ values ranging from 13.01‰ to 17.26‰ VSMOW, with an average of 14.93‰ VSMOW (Fig. 7).

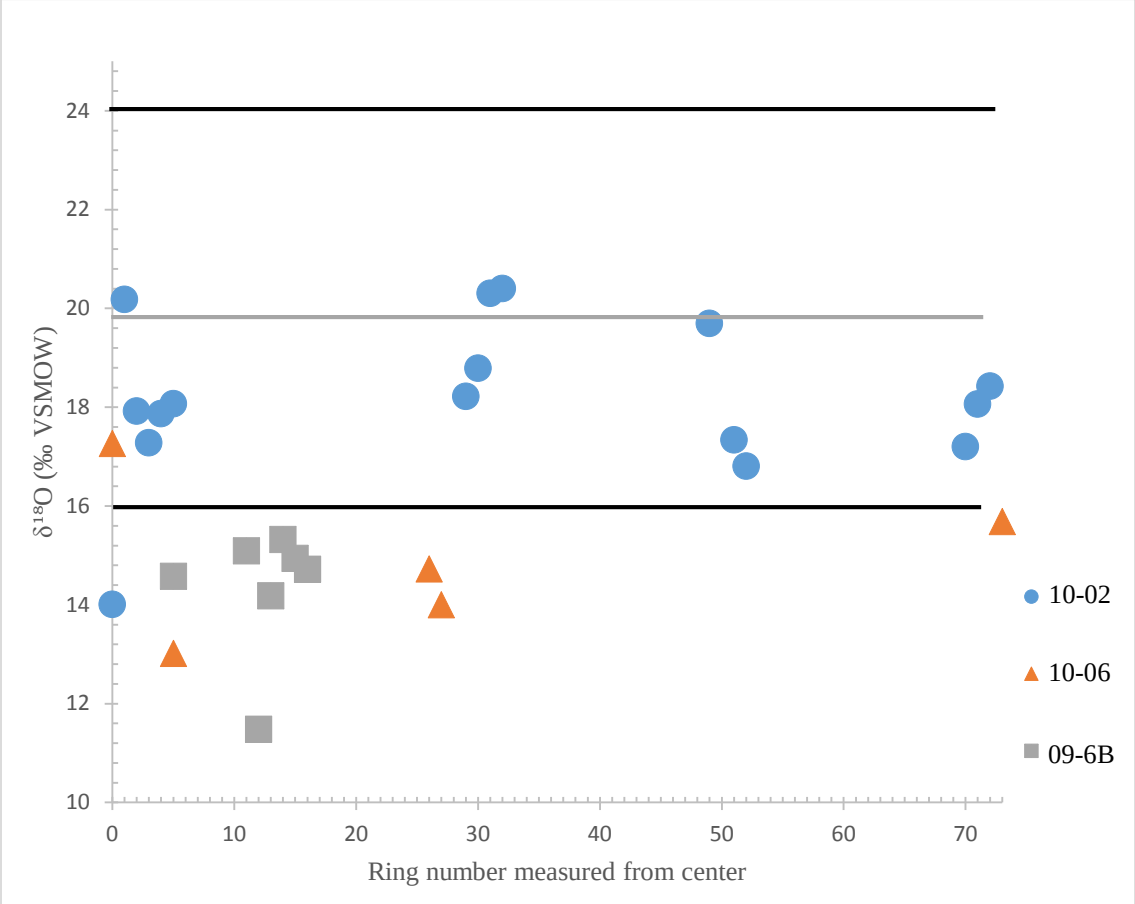

Figure 7. $\delta^{18}O$ values of α-hemicellulose extracts from samples 10-02, 10-06, and 09-6B. Generally, $\delta^{18}O$ values within a single sample are clustered. The range of typical $\delta^{18}O$ values found in high altitude trees from the Pliocene epoch, as described by Csank et al. (2011), is bounded by the thick black lines located at 16.00‰ and 24.00‰ VSMOW, and the mode value of 19.50‰ VSMOW is indicated by the thin grey line.

3.3 FTIR Analysis

Figures 8, 9, and 10 show the FTIR spectra of the three α-hemicellulose samples from select rings: ring 10 from sample 09-6B, ring 49 from sample 10-02, and hemicellulose from recovered from ring 13-39 of sample 10-06. Transmission peaks are found in similar locations consistently across the samples. Peaks with a value of 3333 cm^{-1} - 3341 cm^{-1} describe stretching of –OH groups. Peaks with a value of 2896 cm^{-1} - 2899 cm^{-1} show C-H stretching. Aliphatic esters in the α-hemicellulose

are seen at peaks with values of 1739 cm^{-1} - 1746 cm^{-1}. The peaks with a wavelength of 1643 cm^{-1} - 1652 cm^{-1} are the result of olefinic C=C stretching vibrations. The small peaks at 1427 cm^{-1} and 1428 cm^{-1} conform to the aromatic C=C stretch vibrations within bound lignin. The peaks along the regions that indicate a wavelength of 1023 cm^{-1} - 1030 cm^{-1} represent C-O stretching and deformation bands in the α-hemicellulose. Finally, the small peaks at 583 cm^{-1} - 607 cm^{-1} are ascribed to Si-O-Si stretching in silica (Khandanlou et al., 2013). The absence of an absorption peak at 535 cm^{-1} - 542 cm^{-1} indicates that FeO is not present in any sample, regardless of determined $\delta^{18}O$ value.

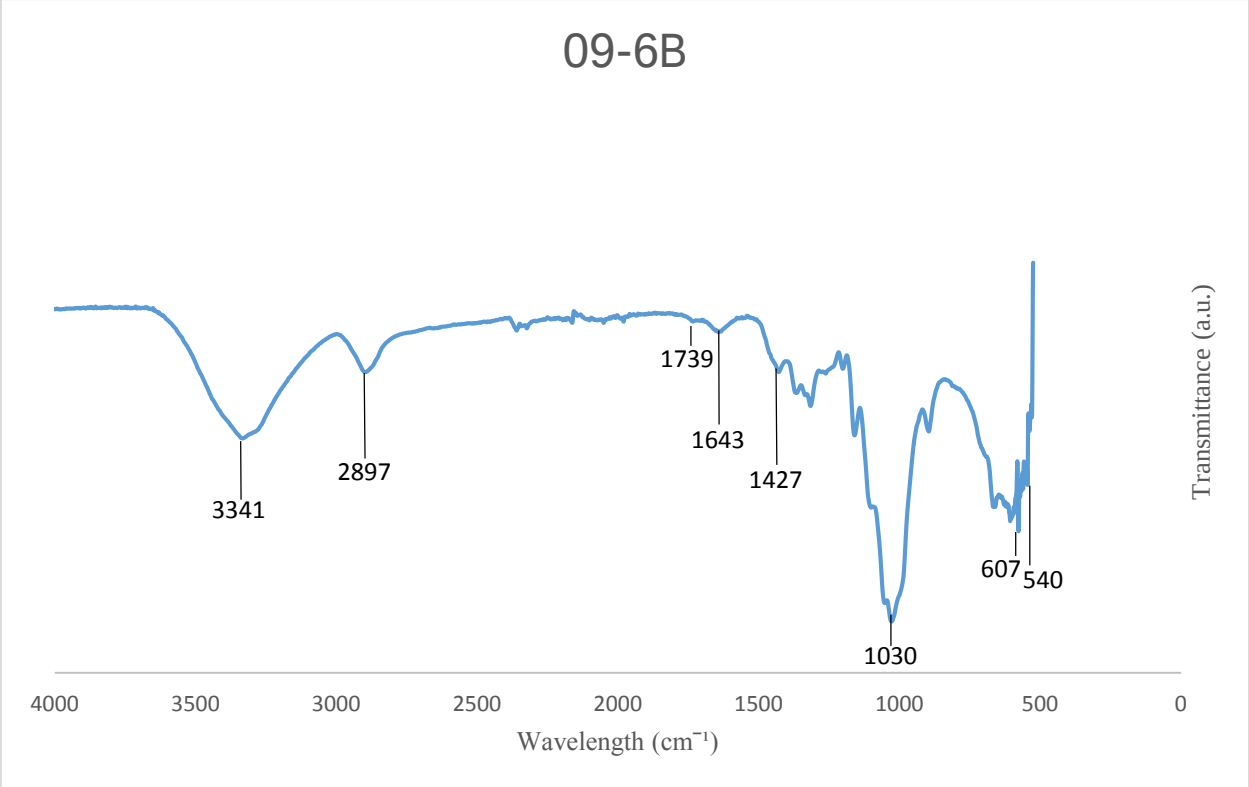

Figure 8. FTIR spectra of sample 09-6B, ring 10.

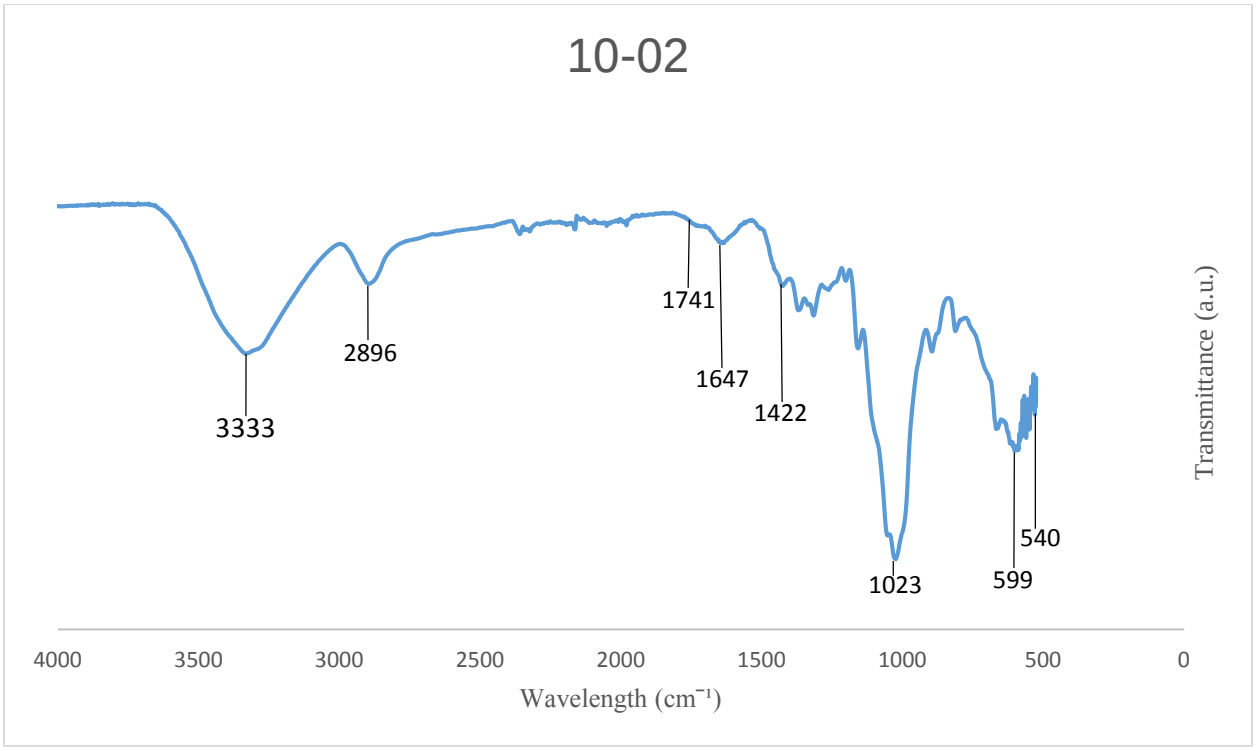

Figure 9. FTIR spectra of sample 10-02, ring 49.

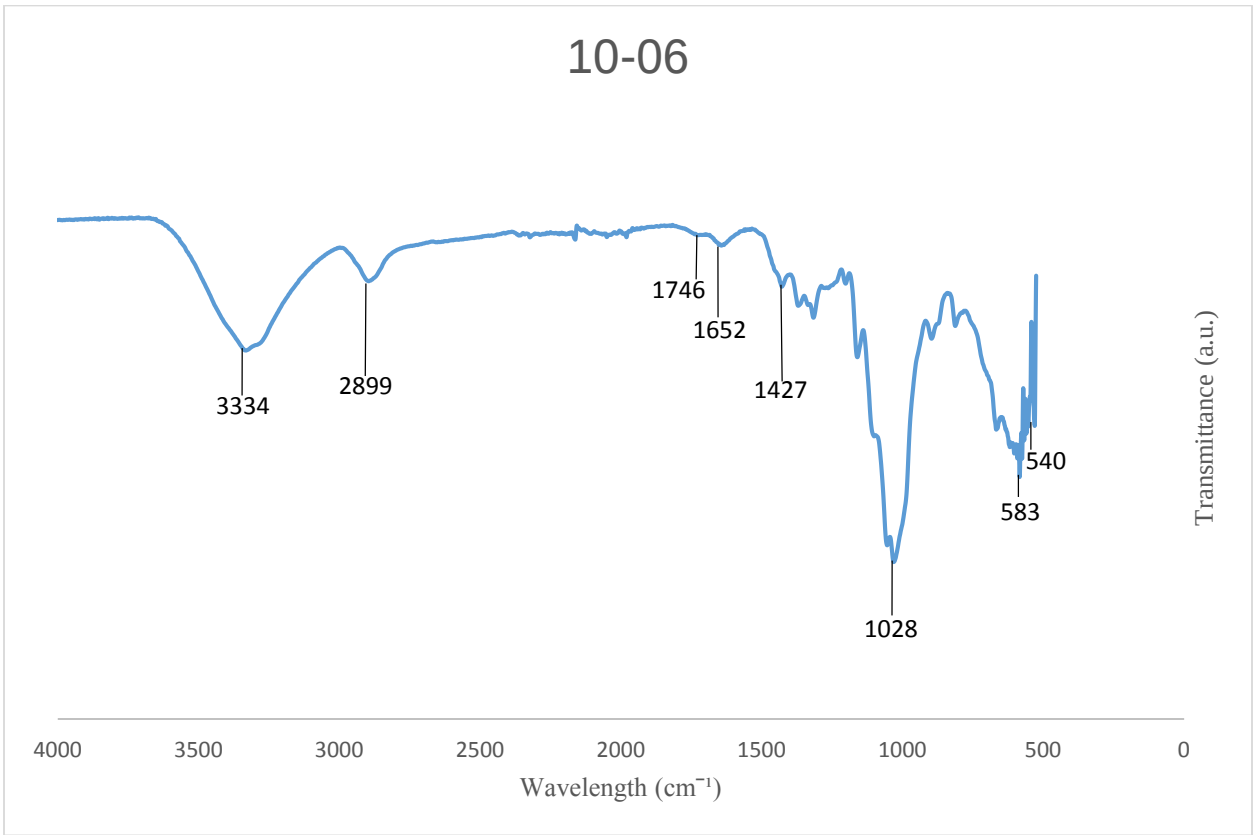

Figure 10. FTIR spectra of sample 10-06, rings 13-39.

3.4 SEM/EDX Analysis

Samples 09-6B, 10-02, and 10-06 underwent further testing for trace elements by SEM/EDX spectroscopy. The results of these tests show insignificant amounts of any trace metal oxides and confirm the results of FTIR spectrometry and suggest that there is no difference between the compositions of the samples determined to have abnormal $\delta^{18}O$ values and that of the sample determined to be typical.

Figures 11, 12, and 13 show the SEM images for the 3 samples of mummified wood at locations where the technician identified potential FeO contamination.

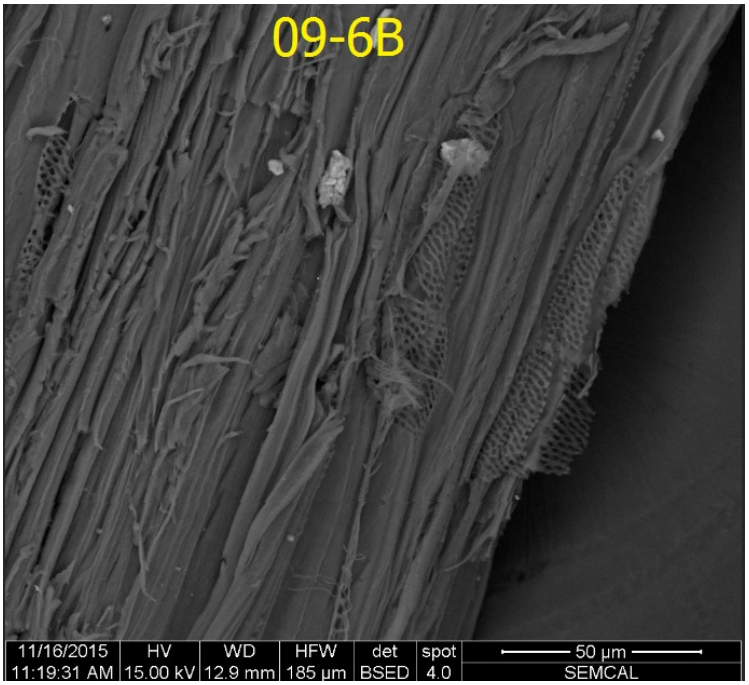

Figure 11. SEM micrograph of sample 09-6B, ring 10. Lighter gray granules were identified as possible FeO contamination.

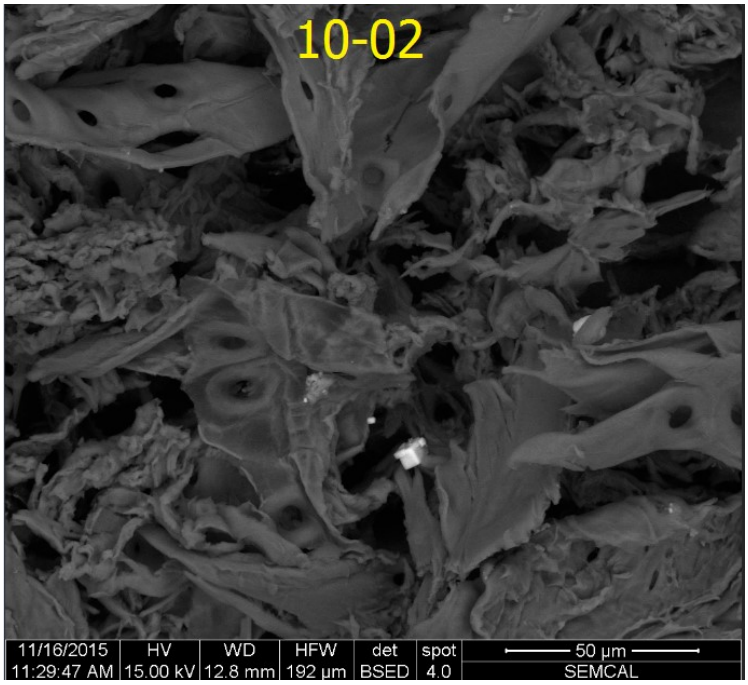

Figure 12. SEM micrograph of sample 10-02, ring 43. Bright white granules were identified as possible FeO contamination.

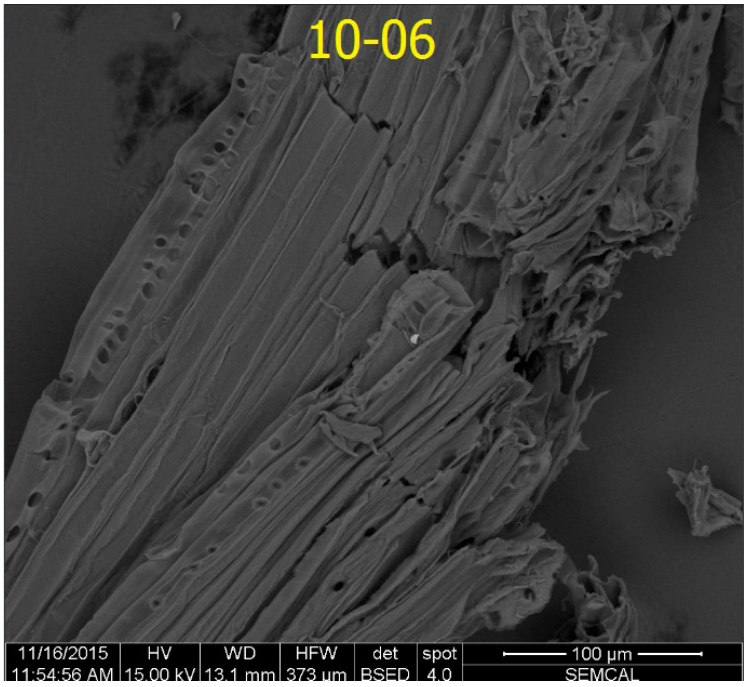

Figure 13. SEM micrograph of sample 10-06, rings 13-39. Light grey granule was identified as possible FeO contamination.

EDX analysis of the potential FeO contamination among the samples resulted in determination that suspected granules were not ferrous metal oxides, but rather silica, aluminum, and salt (Fig. 14, 15, and 16).

09-6B

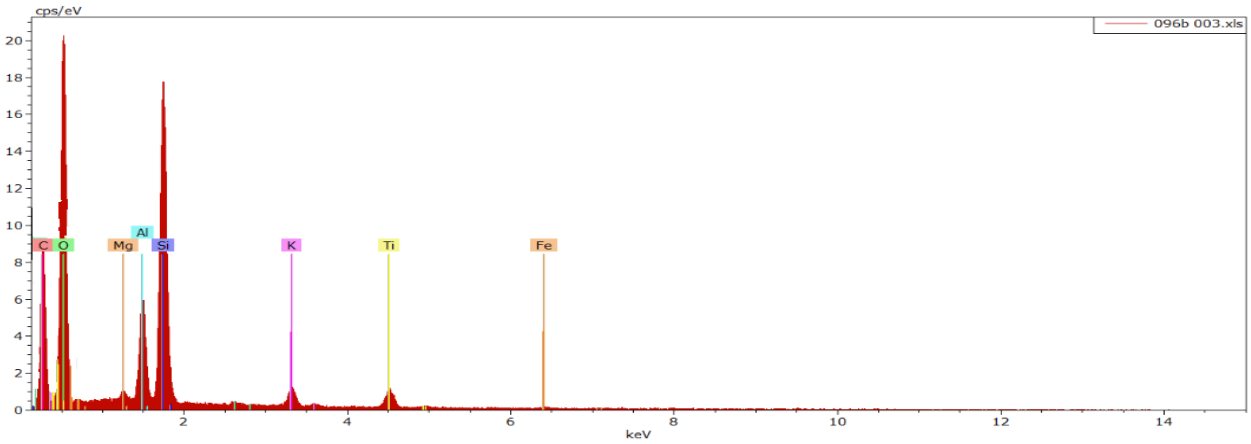

Figure 14. EDX analysis of sample 09-6B, ring 10, showing putative FeO contamination to be silica. Location of expected Fe spike marked.

10-02

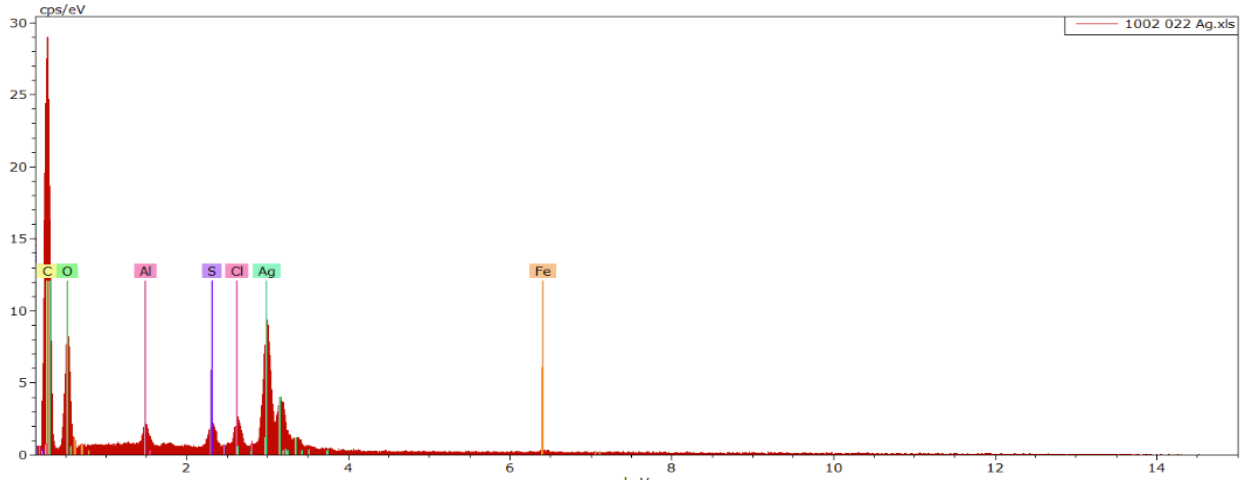

Figure 15. EDX analysis of sample 10-02, ring 43, showing putative FeO contamination to be aluminum. Location of expected Fe spike marked.

10-06

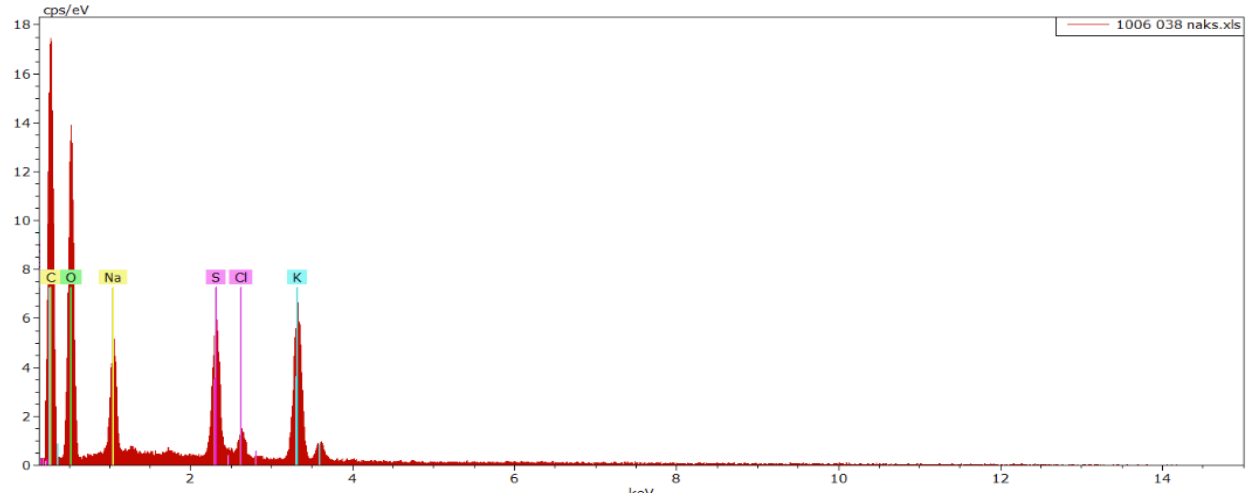

Figure 16. EDX analysis of sample 10-06, rings 13-39, showing putative FeO contamination to be salt.

4. Discussion

Two genera of trees were examined during this study. Two samples were *Betula* (birch; samples 09-6B and 10-06) and a third sample was *Picea* (spruce; sample 10-02). The average tree ring width for all 3 samples is 0.26 mm (Table 2). This is smaller than the width of other Pliocene forest deposits from the high Arctic reported by Ballantyne et al. (2006) for *Larix* (Larch) (0.47 mm, n=3) from Beaver Pond, Ellesmere Island (Fig. 2), and by Csank et al. (2011) for larch (0.39 mm, n=4) from Strathcona Fiord, Ellesmere Island (Fig. 2).

Temperature has been identified as the most influential factor affecting tree growth in boreal forests (Briffa, 2000), with warmer temperatures corresponding to higher growth rate. As such, thin rings represent a relatively cold growing season whereas thick rings represent a relatively warmer growing season. Other factors such as availability of water and nutrients, predation, irradiance, and age can also affect tree ring width (Creber, 1977) but to a lesser extent than temperature. Therefore, the large difference in ring width between the two birch samples may be attributed to warmer growing conditions during the time that 09-6B was alive and relatively cooler growing conditions for 10-06, assuming that other factors are equal. The validity of this assumption may be questioned. None of the tree samples were in growth position when collected and may have been transported prior to deposition (Barker, *pers. comm.*). As such, we cannot rule out the possibility that microclimatological conditions (e.g. water and nutrient availability)

differed among locations where each sampled tree grew and that these factors in combination with regional temperature may have influenced growth rate. However, birch, as a genus, has a relatively narrow ecological tolerance, preferring well-drained acidic soil (Smolander and Kitunen, 2001). This narrow tolerance will regulate variance in microclimatological conditions in favor of well drained acidic soils and the nutrient conditions associated with this growing environment. Therefore, we consider that variance in tree ring width between birch samples is due, primarily, to changes in growing season temperature and that our assumption is valid.

Reed and Harms (1956) showed that there was little difference in the growth rates of Arctic birch compared to Arctic spruce trees. Therefore, similar average growth rates of sample 10-02 (mean = 0.21 mm) and sample 10-06 (mean = 0.12 mm) suggests that temperature may have been similar during the lifespan of both trees. The correlation matrix (Fig. 6) centered each samples peak growth year and bound them by 10 years in each direction. The years surrounding the widest growth rings do not correlate across any of the samples, showing that although 10-02 and 10-06 lived under the influence of similar environmental conditions, none of the trees grew at the same time.

The age for each sample was determined by counting the number for growth rings. In each sample, the tree rings grew too close together near the outer edge to allow us to count the rings. Thus results are reported as a minimum age. The spruce has a minimum age of 102

years. The minimum ages of the birch samples are 54 years (sample 09-6B; Table 2) and 106 years (sample 10-06; Table 2). Sample 09-6B has wider tree rings (mean = 0.42 mm) than sample 10-06 (mean = 0.12 mm). The wider tree rings in sample 09-6B suggests better growing conditions then sample 10-06. While the absence of a correlation between growth pattern between the birch samples suggests that they grew at different times (Fig. 6), the wider annual growth rings in sample 09-6B indicated that it grew under warmer conditions than sample 10-06.

Csank et al. (2011) reported $\delta^{18}0$ levels of α-hemicellulose of Pliocene Arctic larch to have a range of 16‰ - 24‰ VSMOW and a mean of 19.5‰ VSMOW (Fig. 7). The α-hemicellulose extracts from our two birch samples both display oxygen isotope values that have a lower mean (09-6B mean = 14.32‰ VSMOW, 10-06 mean = 14.94‰ VSMOW; Fig. 7). All analyzed tree rings from sample 09-6B are below the minimum expected $\delta^{18}0$ value predicted by Csank et al. (2011; Fig. 7) and in sample 10-06, all but one (pith = 17.26‰ VSMOW; Fig. 7) are below, as well. Analyzed tree rings from the spruce (mean = 18.43‰ VSMOW) displays levels within the range determined typical by Csank et al. (2011) except one (pith = 14.00‰ VSMOW). There is no significant difference in oxygen fractionation among tree species (Battapaglia et al., 2009) so differences in O values among trees result from changes in growing season temperature, as derived from the equation

$$T = 1.9819 \times (\delta^{18}O_{cellulose} (-17- \delta^{18}O_{sw})) - 33.1484 + 2.2333 \times RW$$

where: T is mean annual temperature (MAT (°C)), $\delta^{18}O_{cellulose}$ is the isotopic value of tree ring cellulose relative to VSMOW, $\delta^{18}O_{sw}$ is the isotopic value of the local source water at the site where the tree ring samples were collected, 1.9819, -33.1484, and 2.2333 are constants, and RW is the average ring width of the sample (Csank et al., 2011). The presence of metal oxides as a contaminant in the α-hemicellulose extract may also result in lower O values. While the isotopic value of oxygen in the cellulose of tree rings is dependent on the isotopic composition of the water used by the tree during cellulose synthesis, which in turn in influenced by atmospheric temperature due to Rayleigh distillation effects on precipitation, in regions where the soil is rich in metal oxides, soil water can become enriched in dissolved metals that oxidize during α-hemicellulose extraction and result in abnormally low $\delta^{18}O$ values (Richter et al., 2008).

To determine if FeO contamination is the source of the low $\delta^{18}O$ values seen in sample 09-6B and 10-06, α-hemicellulose extracts were analyzed by FTIR spectrometry. α-hemicellulose from ample 10-02 (spruce) displayed an O value that fell within the range of those reported by Csank et al. (2011) and was used as a comparison against the birch samples that displayed O values that fell outside of the range reported by Csank et al. (2011). Any presence of FeO in the α-hemicellulose extracts would result in increased transmission at 535-542 cm^{-1} (Saikia and

Parthasarathy, 2010) due to stretching of the Fe-O caused by the vibrations of the bond due to infrared radiation absorbance. The FTIR spectra for the samples are similar and composed of peaks associated with stretching vibrations. The vibrations are caused by the effect of the oscillating electric field of the radiation on the polar bonds within the α-hemicellulose, specifically those of the –OH groups, olefinic and aromatic C=C bonds, and C-H bonds. As stated earlier, stretching within FeO molecules, if present, would produce a spike between 535 cm^{-1} - 542 cm^{-1}. A definitive spike in this region is not seen in any of the spectra collected. However, the region surrounding 535 cm^{-1} - 542 cm^{-1} is near several other broad peaks (at 583 cm^{-1} - 607cm^{-1}; Fig. 8-10) associated with Si-O-Si stretching and so the possibility that these broader peaks are masking a FeO spike cannot be ruled out. To reconcile this possibility, we analyzed each sample by SEM/EDX to detect if any FeO is present.

The images produced by the SEM (Figs. 11-13) show bundles of fibrous hemicellulos with small, reflective particles indicating a contaminant. However, these trace amounts of impurities, when analyzed by EDX, (Figs. 14-15) are shown not to be FeO but salts or silica that are most likely the result of the α-hemicellulose extraction procedure. These EDX images, in conjunction with the nearly universal resemblance amongst the FTIR spectra, suggest that FeO is absent in the samples and that lower $\delta^{18}O$ values in the α-hemicellulose extracts in

sample 09-6B and 10-06 result from the composition of the source water when each tree was growing.

After ruling out FeO contamination, the low $\delta^{18}O$ values displayed by sample 09-6B and 10-06 are thought to be the result of climate rather than the presence of FeO. These results expand on the range of O values currently cited for α-hemicellulose from fossil forest deposits in the Arctic by Csank et al. (2011), of 16‰ - 24‰ VSMOW. Other studies have shown a correlation between $\delta^{18}O$ values of tree rings and mean annual temperature, specifically that higher $\delta^{18}O$ values are the result of warmer growing seasons (McCarroll and Loader, 2004, Saurer et al., 2008, and Sidorova et al., 2009). The low values therefore suggest that Pliocene temperature at the deposit from which these samples were gathered was lower than the deposit from which Csank et al. (2011) gathered their samples. Inputting our data into the formula developed by Csank et al. (2011) supports this. In this equation we use the constants derived by Csank et al. (2011) and their value for source water oxygen isotope levels along with our results from oxygen isotope analysis and ring width measurements of sample 09-6B at ring 12, which represents the year with the lowest $\delta^{18}O$ value recorded in our study (Fig. 3; Fig. 7).

$$T = 1.9819 \times (-11.48 + (- 17 - (- 16.3))) - 33.1484 + 2.2333 \times .42$$

This equation produces a MAT for our deposit of -10.82 °C. This result is lower than the range of MAT values reconstructed by Csank et al. (2011)

of -1.4±4.0°C. The lower temperature of our deposit suggests that these trees grew at higher altitudes or at a time during the Pliocene when Artic temperature was colder.

5. Conclusion and Suggestions for Future Works

FeO contamination was not detected in the α-hemicellulose extracts from birch and spruce trees at the Ekblaw A site. As such the α-hemicellulose extracts are sufficiently clean and FeO contamination is not the cause of anomylously low oxygen isotope values and thus useful for calculations of Pliocene temperature at the Ekblaw A site. These lower values indicate a MAT that is ~10 °C colder than MAT reported for Pliocene sites at more southerly Arctic locations. This indicates either a steep latitudinal gradient in MAT, if the Ekblaw A trees coexisted with Csank et al. (2011), or, more likely, that the Ekblaw A trees existed during a time in the Pliocene when MAT was cooling, perhaps in the Late Pliocene during the transition into the current Arctic "ice house" conditions.

It is important to acknowledge that these results are based on results determined by only three fossil tree trunks. These results could be untypical and suggest that more sampling is necessary before an extension of the typical $\delta^{18}O$ range of Pliocene Arctic trees can be made. The addition of more samples may also make it possible to cross date trees from this site which would enable us to assess whether missing rings occur in wood from Ellesmere Island and provide a more accurate timeline for the lifespan of these trees.

Further temperature determination of these samples would be beneficial in bolstering the results of this study. Mean annual temperature could be derived across the lifespan of the tree by using the

methods of Csank et al. (2011) and, with the inclusion of more specimens, a stronger case could be made to extend the temperature range of the Pliocene Arctic. Also, testing of the hemicellulose for carbon isotopes can be used, by following methods outlined by Csank et al. (2011), to determine the temperature of the growing season (June to July) and also to derive relative humidity. These calculations could give further insight into the environmental changes that can be expected in the Arctic over the next century.

References cited

Ballantyne, A. P., Rybczynski, N., Barker, P.A., Harington, C.R., White, D., 2006. Pliocene Arctic temperature constraints from the growth rings and isotopic composition of fossil larch. Palaeogeography, Palaeoclimatology, Palaeoecology 242, 188-200.

Battapaglia, M., Saurer, M., Cherubini, P., Siegolf, R.T.W, Cotrufo, M.F., 2009. Tree rings indicate different drought resistance of a native (*Abies alba* Mill.) and a nonnative (*Picea abies* (L.) Karst.) species co-occuring at a dry site in Southern Italy. Forest Ecology and Management 257, 820-828.

Briffa, K. R., 2000. Annual climate variability in the Holocene: interpreting the message of ancient trees. Quaternary Science Reviews 19, 87-105.

Creber, G.T., 1977. Tree rings: a natural data-storage system. Biological Review 52, 349-383.

Csank, A.Z., Patterson, W.P., Eglington, B.M., Rybczynski, N., Ballantyne, A., 2011. Climate variability in the Early Pliocene Arctic: Annually resolved evidence from stable isotope values of sub-fossil wood, Ellesmere Island, Canada. Palaeogeography, Palaeoclimatology, Palaeoecology 308, 339-349.

Csank, A.Z., Tripati, A., Patterson, W.P., Eagle, R.A., Rybczynski, N., Ballantyne, A., Eiler, J.M., 2011. Estimates of Arctic land surface temperature during the Early Pliocene from two novel proxies. Earth and Planetary Science Letters 304, 291-299.

Green, J.W., 1963. Methods of Carbohydrate Chemistry. Academic Press, New York, NY, pp. 9-21.

Davis, S.J., Caldeira, K., Matthews, H.D., 2010. Future CO_2 emissions and climate change from existing energy infrastructure. Science 329, 1330-1333.

Holland, M.M., Bitz, C.M., 2003. Polar amplification of climate change in coupled models. Climate Dynamics 21.3, 221-232.

Hughes, M.K., Vaganov, E.A., Shyatov, S., Touchan, R., Funkhouser, G., 1999. Twentieth-century summer warmth in northern Yakuita in a 600-year context. The Holocene 9, 629-634.

Karl, T.R., Trenberth, K. E., 2003. Modern global climate change. Science 302.5651, 1719-1723.

Khandanlou, R., Bin Ahmad, M., Shameli, K., Kalantari, K., 2013. Synthesis and characterization of rice straw/Fe3O4nanocomposites by a quick precipitation method. Molecules 18, 6597-6607.

Knutz, P.C., Hopper, J.R., Gregersen, U., Nielsen, T., Japsen, P., 2015. A contourite drift system on the Baffin Bay-West Greenland margin linking Pliocene Arctic warming to the poleward ocean circulation. Geology 43, 907-910.

Loader, N.J., Robertson, I., Barker, A.C., Switsur, V.R.mm Waterhouse, J.S.A., 1997. An improved technique for the batch processing of small wholewood samples to -cellulose. Chemical Geology 136, 313-317.

McCarroll, D., Loader, N. J., 2004. Stable isotopes in tree rings. Quaternary Science Reviews 23, 771-801.

Pachauri, R.K., Allen, M.R., Barros, V.R., Broome, J., Cramer, W., Christ, R., Church, J.A., Clarke, L., Dahe, Q., Dasgupta, P., Dubash, N.K., Edenhofer, O., Elgizouli, I., Field, C.B., Forster, P., Friedlingstein, P., Fuglestvedt, J., Gomez-Echeverri, L., Hallegatte, S., Hegerl, G., Howden, M., Jiang, K., Jimenez Cisneroz, B., Kattsov, V., Lee, H., Mach, K. J., Marotzke, J., Mastrandrea, M.D., Meyer, L., Minx, J., Mulugetta, Y., O'Brien, K., Oppenheimer, M., Pereira, J.J., Pichs-Madruga, R., Plattner, G.K., Pörtner, H.O., Power, S.B., Preston, B., Ravindranath, N.H., Reisinger, A., Riahi, K., Rusticucci, M., Scholes, R., Seyboth, K., Sokona, Y., Stavins, R., Stocker, T.F., Tschakert, P., van Vuuren, D., van Ypserle, J.P., 2014. Climate Change 2014: Synthesis Report. Contribution of Working Groups I, II and III to the Fifth Assessment Report of the Intergovernmental Panel on Climate Change. Geneva, Switzerland, IPCC, 151 p., ISBN: 978-92-9169-143-2.

Reed, J.C., Harms, J.C., 1956. Rates of tree growth and forest succession in the Anchorage-Matanuska Valley area, Alaska. Arctic Institute of North America 9, 239-248.

Richter, S.L., Johnson, A.H., Dranoff, M.M., LePage, B.A., Williams, C.J., 2008. Oxygen isotope ratios in fossil wood cellulose: Isotopic composition of Eocene to Holocene aged cellulose. Geochimica et Cosmochimica Acta 72.12., 2744-2753.

Saikia, B. J., Parthasarathy, G., 2010. Fourier transform infrared spectroscopic characterization of kaolinite from Assam and Meghalaya, Northeastern India. International Journal of Modern Physics 1, 206-210.

Saurer, M., Cherubini, P., Reynolds-Henne, C.E., Treydte, K.S., Anderson, W.T., Siegwolf, R.T.W., 2008. An investigation of the common signal in tree ring stable isotope chronologies at temperatre sites. Journal of Geophysical Research-Biogeosciences 113, G04035.

Serreze, M.C., Walsh, J.E., Chapin III, F.S., Dyurgerov, M., Romanovsky, V., Oechel, W.C., Morison, J., Zhang, T., Barry, R.G., 2000. Observational evidence of recent change in the Northern high-latitude environment. Climate Change 46, 159-207.

Sidorova, O.V., Siegwolf, R.T.W., Saurer, M., Shashkin, A.V., Knorre, A.A., Prokushking, A.S., Vaganov, E.A., Kirdyanov, A.V., 2009. Do centennial tree-ring and stable isotope trends of *Larix gmelinii* (Rupr.) indicate increasing water shortage in the Siberian north? Oecologia 161, 825-835.

Smolander, A., Kitunen, V., 2001. Soil microbial activities and characteristics of dissolved organic C and N in relation to tree species. Soil Biology and Biochemistry 34, 651-660.